Nucleic Acids Research, 1994, Vol. 22, No. 3 479–484

Linkage structures strongly influence the binding cooperativity of DNA intercalators conjugated to triplex forming oligonucleotides

Frank M.Orson[1,2,3,*], Berma M.Kinsey[1,4] and W.Michael McShan[1,2]
[1]Veterans Affairs Medical Center Research Center on AIDS and HIV Infections, [2]Department of Internal Medicine, [3]Department of Microbiology and Immunology and [4]Center for Biotechnology, Baylor College of Medicine, Building 109, Room 226, VAMC, 2002 Holcombe, Houston, TX 77030, USA

Received August 23, 1993; Revised and Accepted November 29, 1993

ABSTRACT

Conjugation of DNA intercalators to triple helix forming oligodeoxynucleotides (ODN's) can enhance ODN binding properties and consequently their potential ability to modulate gene expression. To test the hypothesis that linkage structure could strongly influence the binding enhancement of intercalator conjugation with triplex forming ODN's, we have used a model system to investigate binding avidity of short oligomers conjugated to DNA intercalators through various linkages. Using a $dA_{10}\cdot T_{10}$ target sequence imbedded in a 20 bp duplex, binding avidities of a T_{10} ODN joined to the DNA intercalator 6,9-diamino, 3-methoxy acridine (DAMA) by 8 different 5′ linkages were measured using an electrophoretic mobility shift assay. Although unmodified T_{10} has a very limited capacity for stable binding under these conditions (apparent K_d >250 μM at 4°C), conjugation to DAMA using flexible linkers of certain lengths and chemical compositions greatly enhanced binding (K_d of 1 μM at 4°C). Other linkers, however, modestly enhanced binding or had no effect on binding at all. Thus, the length, flexibility, and chemical composition of linker structures all substantially influence intercalator conjugated oligodeoxynucleotide binding avidity.

INTRODUCTION

The development of sequence specific agents to modulate gene expression has great potential for therapy of genetic, viral, and malignant diseases. Oligodeoxynucleotides (ODN's) can be designed so that they will bind duplex DNA in a sequence specific fashion, forming a DNA triple helix (1, 2, 3, 4). Triple helix structure, ODN design, and potential applications of triplex forming ODN's have been recently reviewed (5, 6). Covalent attachment of acridine derivatives, psoralen, and selected other intercalators has been used previously to enhance binding and biologic activity of triplex forming oligomers [reviewed in (6)]. However, there have been no systematic investigations to evaluate the influence of the chemical structures that link the ODN to the intercalator. To improve linker design, we have used a model system to investigate the effects on triplex formation conferred by oligomer conjugation with a DNA intercalator, using eight different linkers. Our results suggest that the linkage structure, as well as its effective length, has a significant influence on the binding avidity of an ODN for its target duplex.

MATERIALS AND METHODS

Chemicals and oligodeoxynucleotides

Chemicals were purchased from the following sources: Aldrich Chemical Co., Milwaukee, WI (CTPD, DMSO-d_6, anhyd. acetonitrile); Applied Biosystems, Foster City, CA (TETD, DNA synthesis reagents); Fluka Chemical Co., Ronkonkoma, NY (SMP, anhyd. DMF); Glen Research, Sterling, VA (DECP, ST-CP); Pierce Chemical Co., Rockford, IL (SPDP), and Sigma Chemical Co., St Louis, MO (SBA). Syntheses of the acridine derivatives were carried out according to standard methods as indicated in Figure 1. All of the compounds were purified by flash chromatography on silica gel 60, 230–400 mesh (Aldrich), checked by thin layer chromatography on silica gel GHLF plates (Analtech, Newark DE), and their identity was verified by ^{1}H NMR using a 300MHz GE system. Oligodeoxynucleotides were synthesized using standard B-cyanoethyl phosphoramidite chemistry on an ABI 391 DNA synthesizer (Applied Biosystems). Unmodified ODN's were purified after a trityl-on synthesis by reverse phase HPLC chromatography (Waters HPLC system; Millipore Corp., Marlborough, MA) using a Waters Nova-Pak C_{18} column (3.9×300 mm) and a gradient of 5% to 55% acetonitrile in 0.01M triethylammonium acetate, pH 7.4 over 25 m. The ODN's were then detritylated and repurified by two additional rounds of HPLC chromatography. The conjugated ODN's were prepared as described below and purified by two

*To whom correspondence should be addressed at: Building 109, Room 226, Veterans Affairs Medical Center, 2000 Holcombe Boulevard, Houston, TX 77030, USA

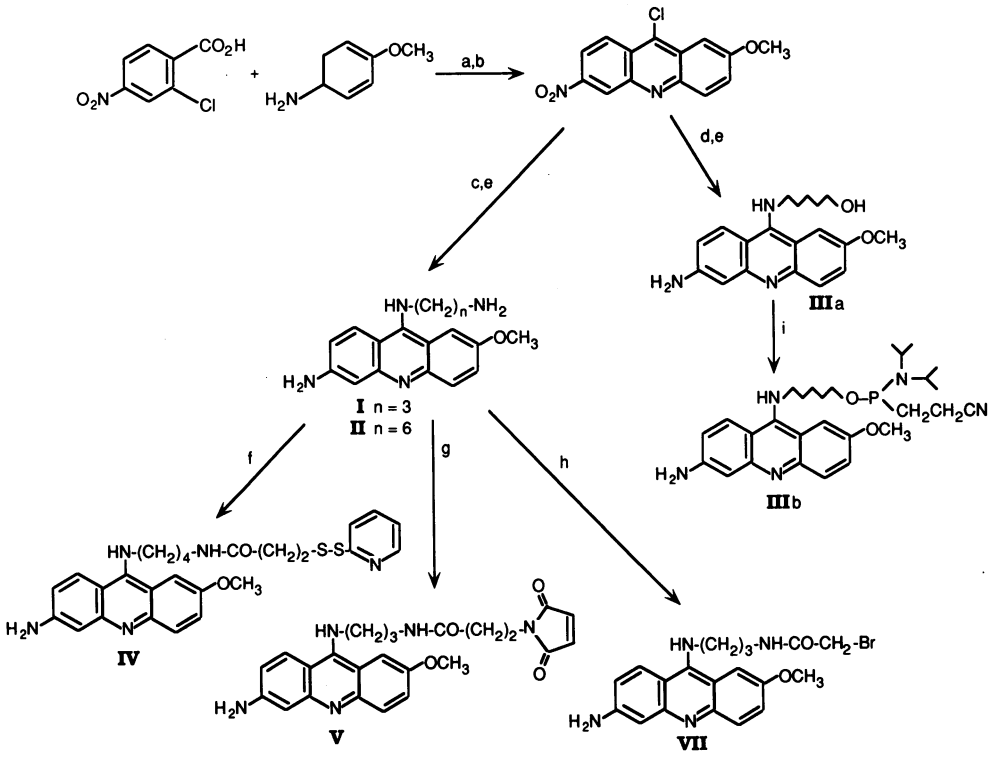

Figure 1. Synthesis scheme of intercalator and linkers. (**a**) Cu, CuO, K_2O_3/ 2-ethoxyethane, reflux 3h (25). (**b**) $POCl_3$/reflux 2h (26). (**c**) $H_2N(CH_2)_nNH_2$/phenol, 80–120°C, 2h (27). (**d**) $H_2N(CH_2)_5OH$/phenol, 80–120°C, 2h (27). (**e**) $SnCl_2$/HCl, reflux 1h (28). (**f**) SPDP/MeOH, 1h, room temperature. (**g**) SMP/MeOH, 1h, room temperature. (**h**) SBA/MeOH, 1h, room temperature. (**i**) CTPD, diisopropylamine·hydrotetrazolide/CH_3CN (29).

rounds of HPLC chromatography using either the system or a Whatman Partisil 10 ODS-2 prep column with 0.01M ammonium acetate and the same acetonitrile gradient. Concentrations were determined by absorbance at 254 nm using the calculated molar extinction coefficient for each oligonucleotide (7).

Linkage of DAMA derivatives to T_{10} ODN's

The ODN conjugates **1** and **2** (Figure 2) were prepared after a standard 1 μmol trityl-off synthesis was done on the DNA synthesizer. For conjugate **1**, the synthesis cartridge containing the controlled pore glass (CPG) beads with the T_{10} ODN still attached was removed from the machine. The beads were incubated with a solution of 50 mg CDI (8) in 1 mL dry acetonitrile by gently passing the solution through the cartridge from time to time between two syringes. After 1 h the beads were washed with acetonitrile and incubated as above for 1 h with a solution of 2 mg compound **I** dissolved in 500 μL dry DMF. The beads were washed with DMF and acetonitrile, removed from the cartridge and incubated overnight with 1 M Na_2CO_3. The solution was filtered and the solvent evaporated. The ODN was resuspended in a small volume of water and desalted on a NAP-5 column, which removed some of the free acridine derivative. The functionalized ODN **1** was purified by HPLC.

ODN conjugate **2** was prepared from **II** by essentially the same method, except 1 mg of **II** was dissolved in 100 μL of DMSO-d_6.

ODN conjugate **3** was prepared using **IIIb** on the DNA synthesizer but lengthening the time of the phosphoramidite coupling step to 1 h. The beads were removed from the cartridge

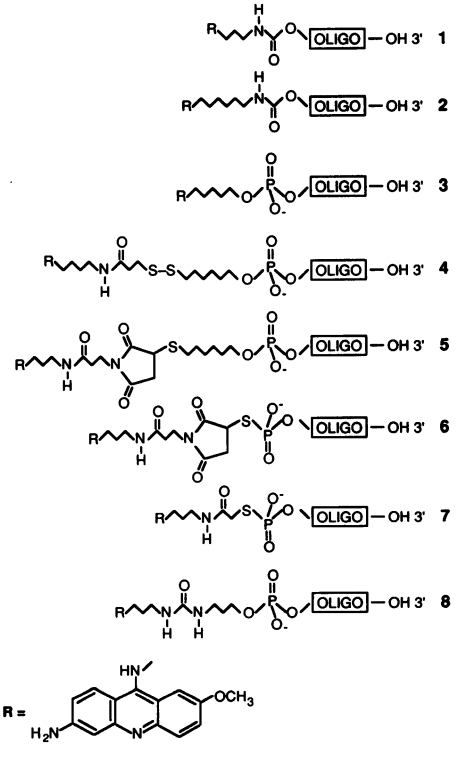

Figure 2. DAMA to oligonucleotide linkage structures. The chemical structures of the various linkages of DAMA to oligonucleotides used in this work are shown. The linker in **3** has been used in other published studies (6, 17, 18).

and treated with 1 mL 0.4 M NaOH in methanol/water 3:1 overnight (9). The solution was filtered and neutralized with Dowex 50 (pyridinium form), and the solvent evaporated. After desalting on a NAP-5 column, **3** was purified by HPLC.

For the preparation of **4** and **5**, the C_6-SH derivative of T_{10}-5'-phosphate was prepared using STCP, following the manufacturer's directions. The detritylated 5'-mercaptohexyl-phosphate-T_{10} was eluted from a NAP-5 column previously equilibrated with 0.1 M phosphate buffer pH 7.5 directly into a magnetically stirred solution of 2 mg **IV** in 100 μL methanol. After 2h, the solution was desalted on a NAP-5 column, the solvent evaporated and the conjugate purified by HPLC. Essentially the same procedure was used for the preparation of 5 except that 2 mg of **V** dissolved in 200 μL DMSO-d_6 was used.

For the preparation of **6** and **7**, a T_{10} ODN was made on the synthesizer and 5' phosphorylated with DECP according to the manufacturer's protocol, except that the oxidation step was carried out using a sulfurizing reagent (TETD), again following the manufacturer's instructions. After standard ammonia deprotection and evaporation of solvent, approximately 1 μmol of the 5'-phosphothioate-T_{10} was resuspended in 200 μL 0.1 M triethylammonium acetate pH 6.5 and added to a solution of 2 mg **V** in 50 μL DMSO-d_6. After 1 h, the ODN conjugate was desalted on a NAP-5 column and purified by HPLC. For 7, the 5'-phosphothioate-T_{10} was resuspended in 100 μL water and 50 μL 5% $NaHCO_3$ and 2 mg **VII** in 150 μL DMSO was added. After 2 h at room temperature. and 1 h at 55°C, the solution was desalted on a NAP-5 column and the conjugate **7** was purified by HPLC.

For the preparation of **8**, the 2-cyanoethyl-N,N-diisopropyl-phosphoramidite of N-FMOC-3-aminopropanol was synthesized (10), dissolved in acetonitrile to form a 0.1 M solution and used in the standard way on the DNA synthesizer except that the coupling step was extended to 15 m. The CPG beads were removed from the cartridge and incubated for 5 m with 500 μL piperidine in a small column equipped with a frit and a stopcock. The piperidine was filtered off and the beads were washed several times with methanol and dried in a gentle stream of air. The beads were then incubated with a solution of 100 mg CDS in 1 mL DMF for 1 h with gentle shaking. The beads were washed with methanol and incubated overnight with 2 mg of compound **I** in 1 mL methanol. Deprotection was accomplished by several hours incubation with 0.4 M NaOH in methanol/water 3:1. The solution was filtered, neutralized with pyridinium Dowex 50, and the solvent was evaporated. The ODN conjugate mixture was resuspended in water, desalted on NAP-5 and purified by HPLC.

Electrophoretic mobility shift assay

These assays were performed with modifications of the methods previously described (11). In brief, control and specific target duplexes (Figure 3) were prepared from synthetic ODN's by annealing and subsequent purification of the duplex by hydroxyapatite chromatography (12), using a 1−500 mM sodium phosphate (pH 7.4) linear gradient. The target duplex had 7 basepairs extending from the 5' end of the $dA_{10}\cdot T_{10}$ oligomer binding region (almost 3/4 of a helical turn), to provide sufficient potential intercalation sites for the DAMA-linker structures when conjugated to T_{10}. The control duplex was sufficiently large (64 basepairs) to contain a wide sequence distribution of potential nonspecific intercalation sites. For triplex forming ODN's with sufficient avidity (< 30 μM K_d), a constant concentration of

```
dA10·T10 Target Duplex:    3'-CTTGAACTTTTTTTTTTGGA
                           5'-GAACTTGAAAAAAAAAACCT
Conjugated Oligomer:          DAMA-L-TTTTTTTTT-3'

Control Duplex:
5'-TCAACGGCAGGGGAATCTCCCTCTCCTTTTATGGGCGTAGTGAAGAAAGGATTCATAAATGAAG-3'
3'-AGTTGCCGTCCCCTTAGAGGGAGAGGAAAATACCCGCATCACTTCTTTCCTAAGTATTTACTTC-5'
```

Figure 3. Conjugated oligonucleotides and duplex target sequences. The sequences of the $dA_{10}\cdot T_{10}$ duplex target sequence and the 64mer control duplex sequence are shown. A T_{10} oligonucleotide with DAMA conjugated by a linker (L) to the 5' terminus is shown in parallel orientation. The chemical composition of the linkage structures and the structure of the acridine deriviative used in these studies are shown in Figure 2.

oligonucleotide (2 μM) was added to the tubes, which contained increasing concentrations of target duplex in binding buffer [10 mM Tris (pH 7.8), 10 mM $MgCl_2$, 10% sucrose]. For low avidity (> 30 μM K_d) ODN's, 10 μM duplex was added to a series of tubes, and then increasing concentrations of oligomer were added, from 20 to 200 μM. Initial experiments established that for these ODN's and targets, maximal binding was achieved within a 30 min preincubation period (data not shown) at the specified temperatures. Samples were then loaded into wells of a 16% polyacrylamide gel (19:1) in a 90 mM Tris/Borate buffer (pH 7.8) containing 10 mM $MgCl_2$. Electrophoresis at 10 V/cm was performed in a waterbath at the desired temperature for 3−4h. The gels were photographed wet under 254 nm UV illumination without staining to demonstrate DAMA-oligonucleotide band shifts. The target duplex migration position was documented by UV shadowing for each gel (13, 14). Fo experiments with unconjugated T_{10}, the oligonucleotide was radiolabelled with ^{32}P for subsequent autoradiography, and UV shadowing was used to document target duplex migration position. For oligonucleotides with binding avidities in the 10^6 L/M range, the nominal K_d was estimated by the formula $K_d = (O\times D)/T$, where O, D, and T represent, respectively, the concentrations of oligonucleotide, duplex, and triplex (11, 15, 16). When O = T, i.e., when half the added oligomer is bound (estimated from visual inspection of the gel under UV illumination), the nominal K_d is equal to the concentration of the residual duplex (see further discussion in Results section). Repeated measurements for intercalator linked oligomers demonstrated reproducible apparent K_d's with the same relative binding efficiency. For poorly binding ODN's (K_d >50 μM), an approximate K_d was estimated based on the apparent distribution of bound versus unbound oligomer at the highest level of binding, using the same equation.

RESULTS

Triplex formation with oligonucleotides conjugated to DAMA

This research compared the influence of several different linkage structures on binding avidity in a model system for triple helix formation. Figure 2 illustrates the 8 linkages used in these experiments. These linkage structures were chosen on the basis of their synthesis feasibility, stability during ODN purification, and structural features that could influence triple helix formation. The carbamate linkages in **1** and **2** differ only by the length of the aliphatic chain attached to the DAMA 9-amino group. Similarly, **6** differs from **5** by the phosphorothioate bond and the lack of an aliphatic chain between the maleimide and oligomer. The linkers in **2** and **7** both have 9 chemical bonds

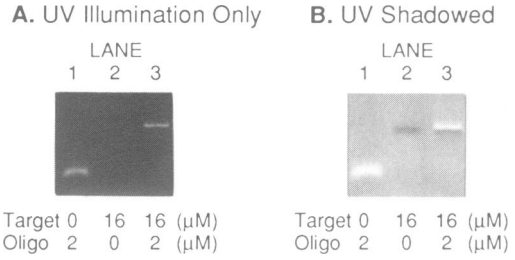

Figure 4. Electrophoretic mobility shift assay with UV shadowed duplex DNA. To illustrate the binding of the DAMA conjugated oligonucleotide to its duplex DNA target, samples containing 2 μM ODN alone, 16 μM $dA_{10}\cdot T_{10}$ duplex DNA alone, or both were electrophoresed on a 16% 19:1 polyacrylamide gel in TBM buffer at 10V/cm for 4 hours at 4°C (lanes 1–3, both panels). Panel A shows a photograph of the unstained wet gel under UV illumination. Lane 1 demonstrates the migration position of unbound ODN alone as a bright band. Lane 2 contained only duplex target and has no fluorescence, while lane 3 illustrates the slowed migration of the ODN bound to the duplex. In panel B, the same gel was photographed with a lightly UV fluorescent mylar sheet placed over the gel. The duplex migration position (lane 2) is shown as a dark band due to the UV absorption of the unstained DNA. Unstained DNA is also visible in lane 3 due to the excess amount of target contained in that sample (16 μM duplex and 2 μM oligonucleotide), illustrating the separation of the double and triple helix DNA's.

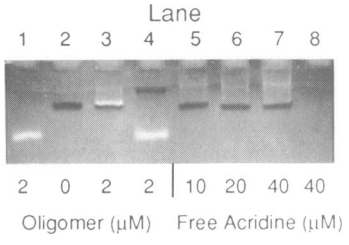

Figure 5. Specificity of 5'DAMA-(**2**)-T_{10} binding to $dA_{10}\cdot T_{10}$ duplex target. To illustrate the specificity of DAMA conjugated ODN binding, samples containing the oligomer with specific or control target duplex, or free DAMA with specific duplex were electrophoresed in a 16% 19:1 polyacrylamide gel in TBM buffer at 10V/cm for 4 hours at 4°C. The photograph (with wells visible at the top of the gel) was taken under UV shadowing conditions (as in Figure 4) to reveal the migration positions of duplex DNA (e.g., lane 2, target duplex alone). ODN conjugate **2** (alone, lane 1) bound to its specific target (lane 3), but did not bind to the control duplex DNA target (16 μM, lane 4). Free intercalator (**III**) at various concentrations in the presence (lanes 5–7) or absence (lane 8) of 16 μM $dA_{10}\cdot T_{10}$ duplex target was not stably bound.

between the 5′ hydroxyl of the ODN and the 9-amino group of the intercalator, differing only by the presence of the phosphate and phosphorothioate bonds.

To examine the binding properties of the T_{10} oligonucleotides to the $dA_{10}\cdot T_{10}$ target duplex, we used an electrophoretic mobility shift assay to detect triple helix formation (11, 15, 16). For DAMA conjugated ODN, binding is readily demonstrated. In Figure 4, panel A illustrates a typical band shift (lane 1: free DAMA-(**2**)-T_{10}, and lane 3: shifted ODN bound to its target duplex). By placing a faintly UV fluorescent sheet of mylar (or a thin glass plate) over the gel, the migration position of the target duplex after electrophoresis can be demonstrated by UV shadowing (lanes 2 and 3), as well as showing the positions of the fluorescent oligomer and triplex (lanes 1 and 3). Figure 5

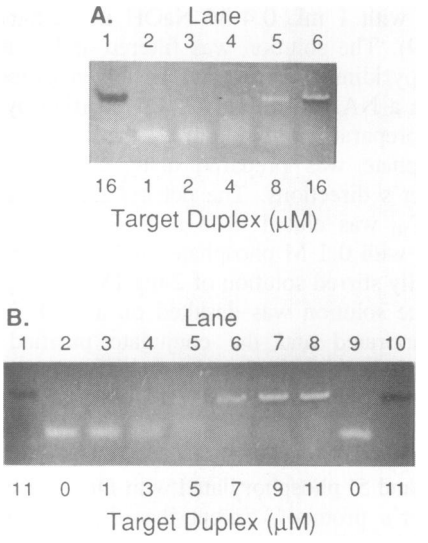

Figure 6. Determination of K_d by electrophoretic mobility shift of 5'DAMA-(**7**)-T_{10} with $dA_{10}\cdot T_{10}$ duplex target. To illustrate the binding of the DAMA conjugated ODN to its duplex DNA target, samples containing $dA_{10}\cdot T_{10}$ duplex DNA alone, 2 μM DAMA-(**7**)-T_{10} alone, or 2 μM oligonucleotide with increasing concentrations of duplex target were electrophoresed on a 16% 19:1 polyacrylamide gel in TBM buffer at 10V/cm for 4 hours at 4°C. As shown in **A**, substantial binding occurred at concentrations of 4 μM and above, and with sufficient excess duplex target, UV shadowing revealed the duplex band below the fluorescent triplex band. A tighter concentration curve (**B**) confirmed that the shift of the ODN occurred between 3 and 5 μM. Both photographs were taken under the same illumination conditions as described in Figure 4.

demonstrates that binding is specific for the appropriate $dA_{10}\cdot T_{10}$ target (lane 3), since the ODN did not bind to other duplex DNA sequences [e.g., a 64 base target duplex (lane 4) from the IL2Ra promoter region which does not contain a long poly dA·poly T sequence].

Without conjugation to an intercalator, however, T_{10} has extremely low avidity under these electrophoresis conditions for the $dA_{10}\cdot T_{10}$ target. In assays performed at 4°C, under conditions in which a 20% shift of radiolabelled oligomer would indicate a nominal K_d of 250 μM, only a slight amount of radiolabelled oligomer was located in the predicted location for a triple helix (data not shown). Previous studies have revealed similar low apparent avidities of short ODN's in both binding assays and biological studies (17, 18). Thus, although T_{10} binding would be predicted to occur in solution at equilibrium (19), the stability of such a triplex is insufficient to detect binding in an electrophoretic mobility shift assay.

Free DAMA binding to duplex DNA during electrophoresis

Although the lack of nonspecific binding to a control duplex target strongly suggests that the DAMA conjugate does not nonspecifically bind the ODN to duplex DNA, we investigated the capacity of free intercalator (**III**) to persistently bind duplex DNA under the conditions of a band shift assay. As shown in Figure 5, no appreciable stable binding of free **III** to duplex DNA occurs at concentrations up to 40 μM (lanes 5–7). However, the gel also demonstrates that binding must have occurred at equilibrium, since **III** (which by itself does not enter the gel, lane 8) is released from the bound state during electrophoresis and diffuses into the gel matrix (smeared fluorescence above the duplex band, lanes 5–7). This is consistent with previously

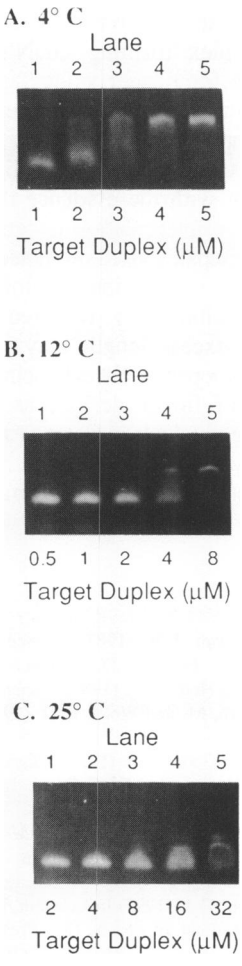

Figure 7. Triplex formation with 5'DAMA-(**2**)-T_{10} at different temperatures. To examine the effects of temperature on the K_d of triplex formation with DAMA-(**2**)-T_{10}, increasing concentrations of $dA_{10}\cdot T_{10}$ duplex target DNA were added to aliquots of a constant amount of ODN (2 μM final concentration), and the samples were electrophoresed on a 16% (19:1) polyacrylamide gel in TBM buffer at the indicated temperatures [4°C (A), 12°C (B), and 25°C (C)].

Table I. Nominal K_d's of 5'DAMA conjugated T_{10} oligonucleotides

Oligonucleotide	Linker Bond No.*	4°C K_d (μM)	12°C K_d (μM)	25°C K_d (μM)
T_{10}	–	>250	ND**	ND
1	6	8	15	ND
2	9	2	4	20
3	8	2.5	5.5	50
4	19	100	ND	ND
5	20	>100	ND	ND
6	13	15	ND	ND
7	9	3	6	35
8	12	1	2	7

K_d's were determined by electrophoretic mobility shift assays. K_d's <30 μM were calculated from this equation under conditions in which 50% of the ODN was bound to its target. For weakly binding oligonucleotides (K_d >30 μM), an approximate K_d was estimated based on the apparent distribution of bound oligomer versus unbound oligomer at the highest level of binding, according to the equation:

$$K_d = (O \times D) / T$$

*The net number of chemical bonds between the DAMA 9 amino nitrogen and the 5' hydroxyl oxygen of the oligonucleotide.
**ND = not done.

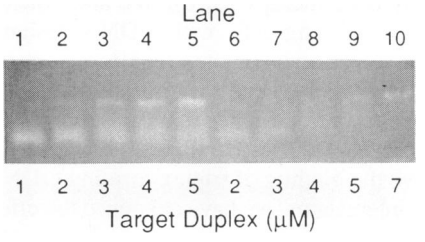

Figure 8. Comparison of two intercalators with the same linker. To examine the binding of two distinct intercalators conjugated by the same linker (**3**) to T_{10}, increasing concentrations of $dA_{10}\cdot T_{10}$ duplex target DNA were added to aliquots of a constant amount of 3-chloro, 6-methoxy acridine-(**3**)-T_{10} or 3,9-diamino, 6-methoxy acridine-(**3**)-T_{10} (2 μM final concentration), and the samples were electrophoresed on a 16% (19:1) polyacrylamide gel in TBM buffer at 4°C. The 3-chloro, 6-methoxy acridine has less intrinsic fluorescence than the 3,9-diamino, 6-methoxy acridine (data not shown), accounting for the differences in band intensities.

reported data which showed that acridine derivatives have K_d's in the 1−2 μM range, but bound and unbound forms are in rapid equilibrium (20). Therefore, this data strongly supports the hypothesis that the conjugated ODN's form relatively stable triple helices due to the cooperative binding of the DAMA and the oligonucleotide.

Binding of DAMA-linker-T_{10} conjugates over a range of temperatures

Conjugation to DAMA with certain linkers resulted in a dramatic enhancement of oligomer binding to the target sequence. As shown in Figure 6A, a band shift determination of the nominal K_d for **7** reveals an approximate 50% reduction in the unbound oligonucleotide band at a duplex concentration of 4 μM (lane 4) with the rest distributed between the triplex band and oligomer released during electrophoresis. Excess unbound duplex target is visible as a dark band in lane 6 just below the fluorescent triple helix band. A tighter concentration curve (Figure 6B) confirmed that the 50% shift would occur between the 3 and 5 μM duplex concentrations (lanes 4 and 5). This results in an estimated effective K_d of 3 μM under these electrophoresis conditions.

To measure binding at different temperatures, band shift assays were performed for **2** at 4°C, 12°C, and 25°C. Nominal K_d's rose with increasing temperature, as expected (Figure 7). The estimated K_d's were 2 μM (4°C), 4 μM (12°C), and 20 μM (25°C). Table I summarizes the results of band shift assays using the eight different linkers tested with the diamino-methoxy-acridine intercalator. Although definitive conclusions cannot be drawn regarding the influence of all aspects of linkage structure, the results suggest that the length of the linker substantially influences binding cooperativity. Relatively longer structures (e.g., **4** and **5**, with 19 and 20 chemical bonds, respectively, between the 5' hydroxyl of the oligonucleotide and the DAMA amino group) bind weakly compared to the shorter linkers. Since **1** (6 bonds) showed less avid binding than **2** (9 bonds), optimal binding cooperativity with the intercalator may require a structure with more than 6 chemical bonds in length.

The reported data suggests that other aspects of chemical structure influence triplex formation. The presence of the 5' phosphate and/or phosphorothioate group appeared to modestly

reduce binding avidity, since the measured K_d's for **2** and **7** (both of which have 9 chemical bonds between the oligomer and the intercalator) showed that **2** (without a phosphate) enhanced binding more effectively. Consistent with these results, a modest decline in stability with a free 5′ phosphate on an unmodified ODN was recently reported (21). ODN conjugate **3**, with a phosphate and a linker length of 8 chemical bonds, also resulted in slightly less effective binding to the target duplex. In addition, the relative flexibility of the linker appeared to influence enhancement of binding avidity. ODN conjugate **8**, for example, with 12 bonds between the oligomer and DAMA, was much more effective than **6** with a linker having 13 bonds and increased rigidity due to the presence of the ring structure. ODN conjugate **4**, on the other hand, while having comparable linker flexibility to **2**, **3**, and **8**, showed no enhancement of binding, likely as a result of its greater length (19 bonds).

DISCUSSION

Design of triplex forming oligonucleotides that can interact selectively with enhancer/promoter regions of specific genes provides a valuable tool for investigation of gene function, and holds the promise of permitting selective manipulation of gene expression by drug therapy (5, 6). We and others have shown that treatment of living cells with ODN's designed to form a triplex in the enhancer/promoter region of a normal gene can specifically suppress the gene's transcription (11, 18). Similarly, ODN's have also been designed that can suppress active proviral replication (16, 17).

To improve the binding of triplex forming ODN's conjugated with a DNA intercalator, we have examined the effects of linkage structure on apparent K_d as measured by an electrophoretic mobility shift assay. Conjugation with DAMA markedly enhances binding from a $K_d > 250$ μM for unconjugated T_{10} to a K_d of 1 μM for conjugate **8**. To permit comparisons of this work with other studies in the literature, we prepared a T_{10} ODN conjugated to 6-chloro, 3-methoxy acridine (18) by the same linkage chemistry as used for **3**, and examined its binding avidity to the same target sequence. The nominal K_d's showed a small, but consistent difference at 4°C (3.5 μM and 2.5 μM, respectively; Figure 8). Therefore, potential enhancements of both linkers and intercalators can be effectively evaluated by electrophoretic mobility shift assays.

Band shift assays have been extensively used to study DNA−protein interactions (22, 23), and have also been used to demonstrate binding of ODN's to their duplex DNA targets (11, 15, 16). We recognize, however, that such an assay does not formally measure K_d in the sense that it can be determined by equilibrium dialysis. Nonetheless, the method can be effectively used as a rapid screening tool for preliminary characterization of the target binding properties of modified triplex forming ODN's. The apparent dissociation constants with a band shift assay may be less than observed at equilibrium in solution due to the release of oligonucleotide from the duplex as the concentration of free ODN in the immediate vicinity of triplex molecules falls during electrophoresis. For practical purposes, therefore, the band shift assay provides a likely upper bound for the K_d of the triple helix. Furthermore, from the point of view of potential biological effects, band shift assays may identify ODN's with lower effective K_d's resulting from slow exchange between the bound and unbound oligomer state. Such slowly exchanging oligonucleotides will likely be more effective in blocking DNA−protein interactions. Therefore, we have used this method as a useful quantitative tool to rapidly screen chemical modifications of triplex forming ODN's in order to select promising structures for further study.

The linkage structures studied in this report demonstrate that both length and composition can strongly influence triple helix formation with intercalator conjugated oligonucleotides. These results are consistent with the evidence that the preferred site for acridine derivative intercalation is between the last 5′ base triplet and the next basepair [based on molecular modeling studies (6) and the properties of free intercalators (24)]. A minimum linker size and flexibility is required to allow effective intercalation, while excess length may permit only transient intercalation without cooperatively enhancing ODN binding. With further refinement of linker design, as well as progress in intercalator and oligonucleotide design, rapid progress in the development of biologically effective oligonucleotides for applications in genetic, infectious, and malignant diseases can be anticipated.

REFERENCES

1. Moser, H.E. and Dervan, P.B. (1987) *Science.* **238**, 645−50.
2. Le, D.T., Perrouault, L., Praseuth, D., Habhoub, N., Decout, J.L., Thuong, N.T., Lhomme, J. and Hélène, C. (1987) *Nucleic Acids Res.* **15**, 7749−60.
3. Hanvey, J.C., Shimizu, M. and Wells, R.D. (1989) *Nucleic Acids Res.* **18**, 157−161.
4. Dervan, P.B. (1989) In Cohen, J.S. (Eds.), Oligodeoxynucleotides: Antisense Inhibitors of Gene Expression. CRC Press, Inc., Boca Raton, FL, pp. 197−210.
5. Gee, J.E. and Miller, D.M. (1992) *Am. J. Med. Sci.* **304**, 366−372.
6. Thuong, N.T. and Hélène, C. (1993) *Angew. Chem. Int. Ed. Engl.* **32**, 666−690.
7. Brown, T. and Brown, D.J. (1991) In Eckstein, F. (Eds.), Oligonucleotides and analogues: A practical approach. IRL Press, New York, pp. 1−24.
8. Wachter, L., Jablonski, J.-A. and Kuzhal, R. (1986) *Nucleic Acids Res.* **14**, 7985−7994.
9. Thuong, N.T. and Chossingol, M. (1988) *Tet. Lett.* **29**, 5905−5908.
10. Nelson, P.S., Sherman-Gold, R. and Leon, R. (1989) *Nucleic Acids Res.* **17**, 7179−7186.
11. Orson, F.M., Thomas, D.W., McShan, W.M., Kessler, D.J. and Hogan, M.E. (1991) *Nucleic Acids Res.* **19**, 3435−3441.
12. Bernardi, G. (1965) *Nature.* **206**, 779−783.
13. Goeller, J.P. and Sherry, S. (1950) *Proc. Soc. Exptl. Biol. Med.* **74**, 381−2.
14. Atkinson, T. and Smith, M. (1984) In Gait, M.J. (Eds.), Oligonucleotide Synthesis: A Practical Approach. IRL Press, Oxford, Engl., pp. 35−82.
15. Cooney, M., Czernuszewicz, G., Postel, E.H., Flint, S.J. and Hogan, M.E. (1988) *Science.* **241**, 456−9.
16. McShan, W.M., Rossen, R.D., Laughter, A.H., Trial, J., Kessler, D.J., Zendegui, J.G., Hogan, M.E. and Orson, F.M. (1992) *J. Biol. Chem.* **267**, 5712−5721.
17. Birg, F., Praseuth, D., Zerial, A., Thuong, N.T., Asseline, U., Le, D.T. and Helene, C. (1990) *Nucleic Acids Res.* **18**, 2901−8.
18. Grigoriev, M., Praseuth, D., Robin, P., Hemar, A., Saison-Behmoaras, T., Dautry-Varsat, A., Thuong, N.T., Helene, C.T. and Harel-Bellan, A. (1992) *J. Biol. Chem.* **267**, 3389−3395.
19. Cheng, Y.-K. and Pettitt, B.M. (1992) *Prog. Biophys. Molec. Biol.*
20. Feigon, J., Denny, W.A., Leupin, W. and Kearns, D.R. (1984) *J. Med. Chem.* **27**, 450−465.
21. Yoon, K., Hobbs, C.A., Walter, A.E. and Turner, D.H. (1993) *Nucleic Acids Res.* **21**, 601−606.
22. Crothers, D.M. (1987) *Nature.* **325**, 464−465.
23. Revzin, A. (1989) *BioTechniques.* **7**, 346−355.
24. Baguley, B.C. (1991) *Anit-Cancer Drug Design.* **6**, 1−35.
25. Cain, B.F., Seelye, R. and Atwell, G.J. (1974) *J. Med. Chem.* **17**, 922−930.
26. Albert, A. and Gledhill, W.J. (1942) *J. Soc. Chem. Ind.* **61**, 159−160.
27. Asseline, U., Thuong, N.T. and Hélène, C. (1986) *Nucleosides and Nucleotides.* **5**, 45−63.
28. Mueller, D.M., Hudson, R.A. and Chuan-pu, L. (1981) *J. Amer. Chem. Soc.* **103**, 1860−1862.
29. Gryaznov, S.M. and Letsinger, R.L. (1991) *J. Amer. Chem. Soc.* **113**, 5876−5877.